Research Article Vol. 12, No. 9 / September 2025 / Optica 1417


# Universal programmable and self-configuring optical filter

David A. B. Miller,[1,*] Charles Roques-Carmes,[1] Carson G. Valdez,[1] Anne R. Kroo,[1] Marek Vlk,[1,2] Shanhui Fan,[1] and Olav Solgaard[1]

[1]Ginzton Laboratory, Stanford University, 348 Via Pueblo Mall, Stanford, California 94305, USA
[2]Department of Physics and Technology, UiT The Arctic University of Norway, NO-9037 Tromsø, Norway
*dabm@stanford.edu

Received 21 January 2025; revised 1 July 2025; accepted 31 July 2025; published 27 August 2025

**Spectral filters are widely used in sensing and communicating with light, such as for separating wavelength channels in communications or sensing the specific spectra of some object or material of interest. The filter function is, however, often fixed, and precise filtering can require precise manufacturing. We propose an approach to integrated optical spectral filtering that allows arbitrary programmability, can compensate automatically for imperfections in filter fabrication, allows multiple simultaneous and separately programmable filter functions on the same input, and can configure itself automatically to the problem of interest, for example, to filter or reject multiple arbitrarily chosen frequencies. The approach exploits splitting the input light into an array of multiple waveguides of different lengths that then feed a programmable interferometer array that can also self-configure. It can give a spectral response similar to arrayed waveguide gratings but offers many other filtering functions, as well as supporting other structures based on non-redundant arrays for precise spectral filtering. Simultaneous filtering also allows an automatic measurement of the temporal coherency matrix and physical separation into the Karhunen–Loève expansion of temporally partially coherent light fields. With this approach, a wide range of spectral operations can be controllably, automatically, and precisely performed by an integrated photonic device with simple programmability.** 

https://doi.org/10.1364/OPTICA.557630

## 1. INTRODUCTION

Optical frequency or wavelength filters [1] are used in a wide variety of applications, including wavelength-division multiplexing in telecommunications and spectroscopy for sensing—for example, of different chemicals or gases. Existing filters and spectrometers include those based on gratings or prisms, multilayer dielectric stacks, resonators, or arrayed waveguide gratings (AWG) [2–8]. Many such filters have little or no programmability after manufacture. Some allow tuning by mechanical movement, e.g., of a grating in a spectrometer. Waveguide array and resonator approaches can be made in integrated photonic circuits, which can allow thermal, optoelectronic, micromechanical, or piezoelectric tuning and other adjustments. Such circuits based on meshes of interferometers can be very programmable [9,10]; "recirculating" interferometer mesh architectures show impressive programmable filtering based on resonating rings [11]. The other major category of interferometer meshes—"forward-only" architectures [9,12–15]—allows simple progressive programming and even self-configuration [9,12–14,16–20], with many successful experimental demonstrations (e.g., Refs. [16–18,20–23]), including as many as 16 mesh inputs [23], but so far only for manipulating spatial fields and modes. Now we show how such forward-only meshes can perform programmable and self-configuring spectral filtering as well as novel measurement and separation of partially coherent light.

Our approach exploits the combination of an array of waveguides of different lengths (as in an AWG) feeding a forward-only interferometer mesh. This opens a wide range of novel and programmable spectral capabilities, some without precedent in conventional filters. Our approach can implement arbitrary filters in a broad set of possibilities; these include multiple-layer filters that give multiple separate programmable filter functions at the same time (so also allowing switching of wavelength channels between outputs). Novel applications include measuring temporal coherence and separating temporally partially coherent fields into their mutually incoherent components. Self-configuration gives automatic tuning to incident wavelengths and allows automatic compensation for some fabrication imperfections, such as small waveguide phase-delay errors from imperfect waveguide lengths. Such compensation opens new architectures including non-redundant array waveguide lengths for precise filtering that otherwise could be particularly sensitive to phase-delay errors in long waveguides. In setting the "center" frequency of a filter, self-configuration can also compensate for imperfection in the power splitting between waveguides and differences in waveguide loss.

## 2. DEVICE CONCEPT

Figure 1(a) illustrates the concept. Light in a single input waveguide is power-split—for example, equally—into an array of multiple waveguides. These waveguides have different lengths $l_p$—for example, each longer than the preceding one by some specific amount $\delta l_o$. The outputs of those waveguides then feed a programmable "forward-only" interferometer mesh. The power splitter and waveguide array can be similar to those of an AWG router, but our approach differs from some previous partially programmable AWG approaches [8] by using a programmable interferometer mesh at the output.

Suppose, for illustration, that the light in the input waveguide is at one specific wavelength or frequency. Because the waveguides are of different lengths, the amplitudes arriving through these different input waveguides (WG1 to WG4 here) to the interferometer mesh will have different phases. (Indeed, if the power splitting is not equal or the waveguides have different losses, the arriving magnitudes may also be different.) So, the mesh then sees a (spatial) mathematical input (column) vector of different complex amplitudes of light at this frequency, with each different vector element appearing as an amplitude in a different one of the mesh input waveguides (WG1 to WG4 here). The phase delays, and hence the vector, will be different for different wavelengths. Essentially, the power splitting and the waveguide array turn different wavelengths of light into different spatial input vectors to the mesh. This key argument allows us to transfer physics and concepts of self-configuring Mach–Zehnder interferometer (MZI) arrays [9,14] from the spatial to the temporal domain.

The simplest category of filters uses a single-layer mesh—i.e., one having just one signal output, as shown in Figs. 1(b) and 1(c), implementing a single, programmable filter function at its signal output. The other "drop" outputs from the single-layer meshes of Figs. 1(b) and 1(c) are shown being dumped into detectors DM1–DM3.

Instead of dumping all the power in the "drop" ports of the MZI interferometers (or other equivalent 2-input, 2-output "2 × 2" blocks [10]) into photodetectors [as shown in Figs. 1(b) and 1(c)], we could instead pass most or all of this power into a second mesh "layer" (Fig. 2). (The "drop-port" detectors of the first layer—DM1 to DM3 in the example in Fig. 1—could be made to be mostly transparent [16], we could tap off a small portion of the power to a separate photodetector [21,22], we could otherwise deduce the power in given waveguides [24], or we could use progressive algorithms based on maximizing the power in the signal output only [12].) This allows the configuration of a second filter function to appear from the signal output of the second such layer. We can similarly continue to stack further such layers for additional such outputs, up to N–1 as in Fig. 2.

Figure 2 shows the device concept with a complete cascade of layers, in this case for a full set of $N$ programmable output filter functions forming a full arbitrary unitary mesh. In Fig. 2, we represent an entire layer as in Figs. 1(b) or 1(c) as a vertical rectangle. Though we could use any unitary mesh that allows programming to route an arbitrary input vector to a signal output, the self-configuring layer architecture [9,12,14] is arguably the simplest and most economical universal approach for each such layer; it also allows simple programmability or self-configuration. Each layer $j$ formally implements a unitary transform $U_j$ between its inputs and its outputs, with the entire mesh matrix $M$ being the product of these.

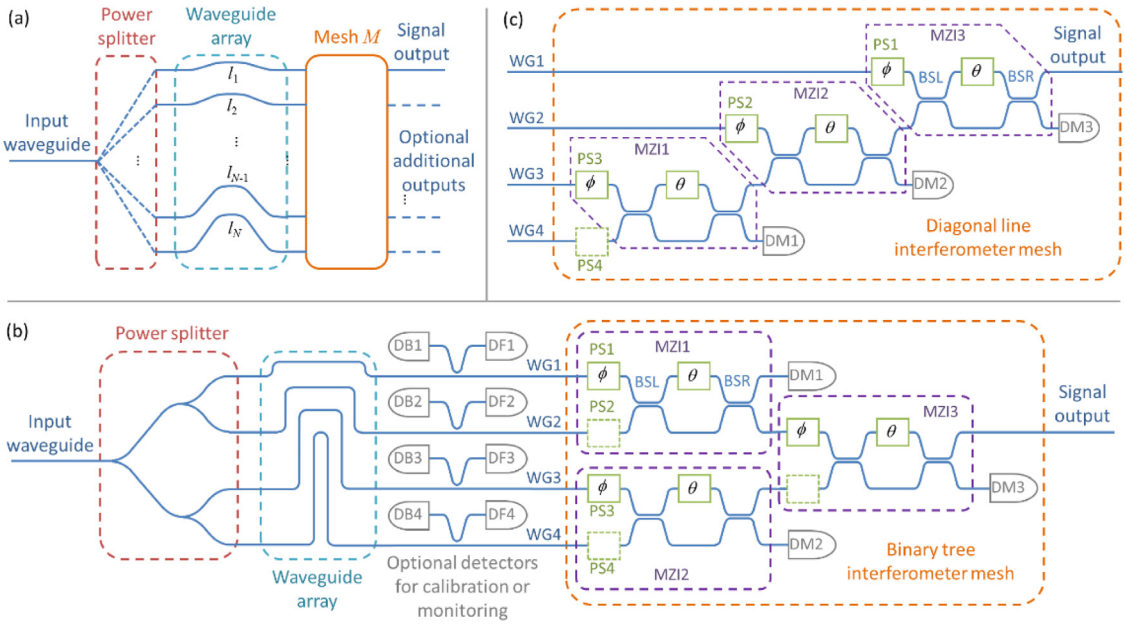


**Fig. 1.** (a) Block diagram with power splitter, waveguide array, and interferometer mesh. (b) Example with a (symmetric) binary tree single-layer interferometer mesh [12,14] with four waveguides. (c) Alternative diagonal line single-layer mesh [12,14]. Square box elements are controllable phase shifters, with at least two required, one "$\phi$" and one "$\theta$," for each Mach–Zehnder interferometer (MZI). (The phase shift values in the "$\phi$" and "$\theta$" shifters in different MZIs will generally be different.) Each MZI also requires two beam splitters, BSL and BSR, that ideally have a 50 : 50 split ratio. Detectors DM1–DM3 can be used to configure the mesh. Optional "tap" detectors DB1–DB3 and DF1–DF3, based on sampling a small amount of the waveguide power, can be used in calibration [14] or for monitoring. Optical phase shifters in dashed boxes are not formally required for full programmability, but PS2 and PS4 in (b) and PS4 in (c) could be convenient, e.g., in tuning the "center" frequency of the filter.

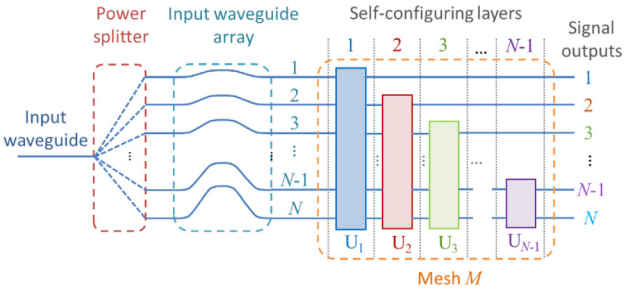


**Fig. 2.** Device with a mesh $M$ formed from $N-1$ successive self-configuring layers to allow multiple simultaneous filter functions at the various different signal outputs, all operating on the same input light.

## 3. DEVICE ANALYSIS

Quite generally, the mesh of Fig. 1(a) multiplies the vector of amplitudes from the waveguide array by a programmable matrix $M$. Multiple-layer interferometer meshes allow the construction of arbitrary matrices $M$ [9]. Programming this matrix, either by calculated setting of interferometer parameters or by self-configuration to the problem of interest, corresponds to programming the spectral response of the system. Such programmability allows a wide and reconfigurable range of filtering behaviors (see Supplement 1, Sections S1 for a detailed analytic approach, S2 for a detailed analysis of a simple filter, and S3 for an extended discussion of mesh matrices and filter functions).

For example, we can make each waveguide $p$ of the $N$ waveguides in the array have relative lengths $\delta l_p$ that are integer multiples $m_p$ of a length $\delta l_o$, i.e., $\delta l_p = m_p \delta l_o$. These will have corresponding relative time delays $m_p \delta t_o$, where

$$\delta t_o = n_g \delta l_o / c, \tag{1}$$

for waveguide group velocity $n_g$ and free-space velocity of light $c$. (This will lead to a filter with a free-spectral range of $\omega_{\mathrm{FSR}} = 2\pi/\delta t_o$ in angular frequency or $f_{\mathrm{FSR}} = 1/\delta t_o$ in conventional frequency.)

We can consider an input (angular) frequency $\delta\omega$ relative to some center frequency. So, for an input amplitude $x(\delta\omega)$ as a function of frequency in the input waveguide, for each output waveguide $q$ we can separately program a filter frequency response $H_q(\delta\omega)$ using settings of the mesh matrix $M$. (We presume $M$ itself is essentially independent of frequency over some reasonable frequency range of interest.) The corresponding signal output in waveguide $q$ as a function of frequency, $y_q(\delta\omega)$, is then

$$y_q(\delta\omega) = H_q(\delta\omega)\, x(\delta\omega). \tag{2}$$

The relative phase delay in input waveguide $p$ will be $m_p \delta\omega \delta t_o$, leading to a propagation factor $\exp(-i\, m_p \delta\omega \delta t_o)$ through that guide. We presume the power splitter leads to relative amplitudes $a_p$ in the array waveguides. (These $a_p$ might all be equal, with a value $\sqrt{1/N}$ for the loss-less case.) Then, for programmed mesh matrix elements $M_{qp}$, these filter functions are given by

$$H_q(\delta\omega) = \sum_{p=1}^{N} a_p M_{qp} \exp\left(-i\, m_p \delta\omega \delta t_o\right), \tag{3}$$

for the signal output waveguide $q$. Formally, we can view this as an expansion of each desired function $H_q(\delta\omega)$ on the orthogonal basis (normalized over a free-spectral range),

$$h_p(\delta\omega) = \sqrt{\frac{\delta t_o}{2\pi}} \exp\left(-i m_p \delta\omega \delta t_o\right), \tag{4}$$

with the required matrix elements $M_{qj}$ evaluated by premultiplying by $h_p^*(\delta\omega)$ and integrating over a free-spectral range, i.e.,

$$M_{qj} \equiv \frac{1}{a_j} \sqrt{\frac{\delta t_o}{2\pi}} \int_{-\pi/\delta t_o}^{\pi/\delta t_o} \exp\left(i m_j \delta\omega \delta t_o\right) H_q(\delta\omega)\, \mathrm{d}(\delta\omega). \tag{5}$$

Equivalently, we are projecting $H_q(\delta\omega)$ onto this orthogonal basis $h_p(\delta\omega)$, a basis that we choose by the design of the lengths of the waveguides in the array. With these definitions

$$\sum_{j=1}^{N} \left|a_j M_{qj}\right|^2 = \delta t_o \int_{-\pi/\delta t_o}^{\pi/\delta t_o} \left|H_q(\delta\omega)\right|^2 \mathrm{d}(\delta\omega). \tag{6}$$

Though Eq. (5) is like establishing a Fourier coefficient for a Fourier-series expansion, in general we call $h_p(\delta\omega)$ just a "Fourier-like" basis because the $m_p$ in successive waveguides are not necessarily successive integers, and there is only a finite number $N$ of such basis functions. If the $m_p$ are successive integers (as in a typical AWG), then Eq. (3) is like a conventional Fourier-series expansion, except only over a finite basis or set of frequencies. (In a conventional Fourier series, the summation as in Eq. (3) would be from $p = -\infty$ to $+\infty$ with $m_p = p$.)

Any filter response $H_q(\delta\omega)$ that is formed from linear superpositions of these Fourier-like basis functions $h_p(\delta\omega)$ is possible. So, a design procedure for a desired filter function $H_q(\delta\omega)$ is (i) evaluate the necessary matrix elements $M_{qj}$ as in Eq. (5), and (ii) deduce the necessary mesh settings to implement these matrix elements.

Note, of course, that only filter functions that can be written as a superposition of these basis functions $h_p(\delta\omega)$ can be exactly implemented by the device, and those basis functions are set by the choice of waveguide lengths. Otherwise, this approach still gives the best approximation (in a "least squares" sense) to the filter design that the device can implement.

## 4. SINGLE-LAYER FILTER

One simple and useful mesh is a single self-configuring layer of MZIs [12,14]. This can be made from a (symmetric) "binary tree" as in Fig. 1(b) or a "diagonal line" of interferometers as in Fig. 1(c), or, indeed, hybrids of these two approaches [14]. For coherent light at a specific frequency, such self-configuring layers can be automatically and progressively configured to direct all the power from any given input vector of amplitudes at that wavelength to their one "signal" output. For example, in the binary tree, we can automatically configure the first (upper) interferometer MZI1, by adjusting its $\phi$ phase-shifter PS1 to minimize the power in its output detector DM1, and then subsequently adjusting its $\theta$ phase shifter to further minimize that same power. With 50:50 beamsplitters in the interferometers, this will result in zero power in the detector DM1. We can simultaneously perform the same kind of power minimization in the second (lower) interferometer MZI2, using detector DM2. Subsequently, we can perform a similar power minimization in the third interferometer MZI3 (in a second "column" of interferometers) using detector DM3. The result is that all the input power is routed to the signal output of the mesh. For the "diagonal line," Fig. 1(c), a similar minimization of one MZI after another also routes all power at this wavelength to its signal output. This progressive approach is easily generalized to larger

binary trees with more input waveguides and "columns" of interferometers, to larger diagonal lines, or to other self-configuring layer architectures [14].

This progressive configuration by single-parameter power minimizations gives the "self-configuring" name [9,12], but such layers can also be defined topologically [14,15] through the property that each input to such a "layer" connects to the layer's signal output by only one path through the $2 \times 2$ blocks or interferometers in the layer.

Hence, this spectrometer or filter will have configured itself to route all the light at this wavelength to the signal output, making a self-configuring filter for this wavelength. It is also possible to perform self-configuration just by progressively maximizing the power at the signal output [12–14], so multiple embedded detectors are not essential. These "single-layer" self-configuring mesh architectures are equivalent to those of the self-aligning beam coupler [12] for spatial modes.

Note that no calibration of the device is required for this operation. Unlike a simple fixed AWG device [6,25], this approach is tolerant of waveguide lengths not being perfectly correct—small length errors are automatically compensated by the mesh phase shifters—and of having possibly different losses; with 50:50 beamsplitters in the MZIs, all the power at that input wavelength that arrives at the ends of the waveguides will still be routed to the signal output. "Perfect" MZI approaches [13,26] allow MZIs with imperfect fabricated beamsplitter ratios to give the same behavior. Note, incidentally, that the self-configuration and calibration algorithms for the mesh do not rely on any specific responsivity in the photodetectors used as long as they have approximately linear response to power; only power maximization or minimization is required for self-configuration and only relative power measurements in a specific signal output are required for phase-shifter calibration.

Once set up in this way, the precise form of the filter function for other input wavelengths depends on the actual lengths (and possibly losses) of the different waveguides in the array, but this function is easily calculated (see Supplement 1, Section S1). With equal power splitting, equal loss in all waveguides and equally spaced waveguide lengths—what we could call a "simple" filter—the filter function is the same as that of an AWG router from any one input to any one output, with the additional benefits of automatic compensation for minor phase errors in waveguide fabrication through the self-configuration process, and simple self-configuration to any desired "center" wavelength. Note that, at least for perfect MZI behavior, the self-configuration process guarantees that all the power emerging at a given wavelength from the waveguides into the mesh is routed to the signal output, giving automatic alignment of the filter to that wavelength, regardless of the lengths of the various waveguides or of different losses or powers in them, or of errors in the power splitting into the waveguides. In that specific sense, this approach is particularly tolerant to fabrication variations in the waveguides. Variations in power splitting and in waveguide loss can also be directly compensated by using a controllable power splitter (see Supplement 1, Section S5).

Note, too, that, unlike a conventional AWG router, the "center" frequency of this filter can be tuned simply, e.g., by using the phase shifters PS1 to PS4 in Fig. 1. All the phase shifters in such meshes can be calibrated by relatively simple progressive algorithms with some reference input at one known frequency or wavelength, especially if the backward sampling detectors, e.g., DB1–DB4 in Fig. 1, are included [14]. Such calibration means any specific filter function as in Eq. (3) can also be directly programmed into the mesh. (See Ref. [14] Supplement 1 for a comprehensive analysis of MZI blocks and programming a self-configuring layer to collect a given vector or, equivalently in the present case, set a specific frequency response $H(\delta\omega)$.)

Figure 3(a) shows calculated results for the frequency response of a simple filter based on the approach of Fig. 1, but with an array of 16 waveguides with successive waveguides longer than the previous one by a length increment of $\delta l_o = 16.51$ μm (as in an AWG). These waveguides feed a 16-input self-configuring layer, such as a 16-input symmetric binary tree. (Such a binary tree would have 8 MZIs in a first column, 4 in a second, 2 in a third, and 1 in a fourth.) In this example, the filter is set up to collect all of one specific frequency, as in the peak of the $\gamma = 0$ curve of Fig. 3(a), showing a frequency response similar to that of one port of an AWG.

For our example calculations, we presume a silicon strip waveguide 500 nm wide by 220 nm tall, for which we estimate a group index of $n_g = 4.05647$ near a "center" wavelength of 1550 nm. The chosen length increment $\delta l_o = 16.51$ μm gives a free-spectral range of 4.4665 THz, slightly larger than the width of the telecommunications C-band. (See Supplement 1, Section S1 for a detailed discussion.)

Once set up for any given frequency, such a filter can be tuned by adding phase increments to the phase shifters at each mesh input, e.g., to the phase shifters PS1–PS4 in Fig. 1. With our presumed waveguides whose lengths differ by an integer multiple $m_p$ of the increment $\delta l_o$, we choose a phase "tilt" number $\gamma$ between 0 and $2\pi$ to add a phase delay,

$$\delta_p = m_p \gamma, \tag{7}$$

to each of the "input" phase shifters, e.g., PS1–PS4 in Fig. 1. In this way, we can tune the filter over its complete spectral range. (In practice, one would subtract any integer multiples of $2\pi$ from the phase $\delta_p$ to get a physical phase shift within a $2\pi$ range for an actual phase shifter.) Figure 3(a) shows this tunability with a set of example values for $\gamma$. One simple way of tuning like this would be to heat up the entire set of waveguides uniformly, relying on the temperature dependence of refractive index in the waveguide material; longer waveguides will acquire proportionately longer phase additions $\delta_p$ as needed in Eq. (7).

Note that, typically, the design of such interferometer meshes themselves is such that both path lengths to any points where pairs of beams interfere inside the mesh are essentially equal, as are all total path lengths from any input to any output; as a result, the mesh itself and the corresponding matrix $M$ are nominally non-dispersive except for dispersion in beamsplitters and in wavelength-dependence of phase shifts. Hence, at least for moderate bandwidths, the performance of the device can be dominated by the different lengths of the waveguide elements, allowing a simple design. So, we neglect any other dispersion of the mesh in our calculations for simplicity; any such additional known dispersion could be straightforwardly included in a numerical analysis of the device operation; equivalently, we presume the matrix $M$ does not itself depend on wavelength.

This single-layer filter, especially with constant length (or, equivalently, time delay) increments between the waveguides in the array, can be viewed as a tapped-delay-line, transversal, or (non-regressive) moving-average finite-impulse-response filter

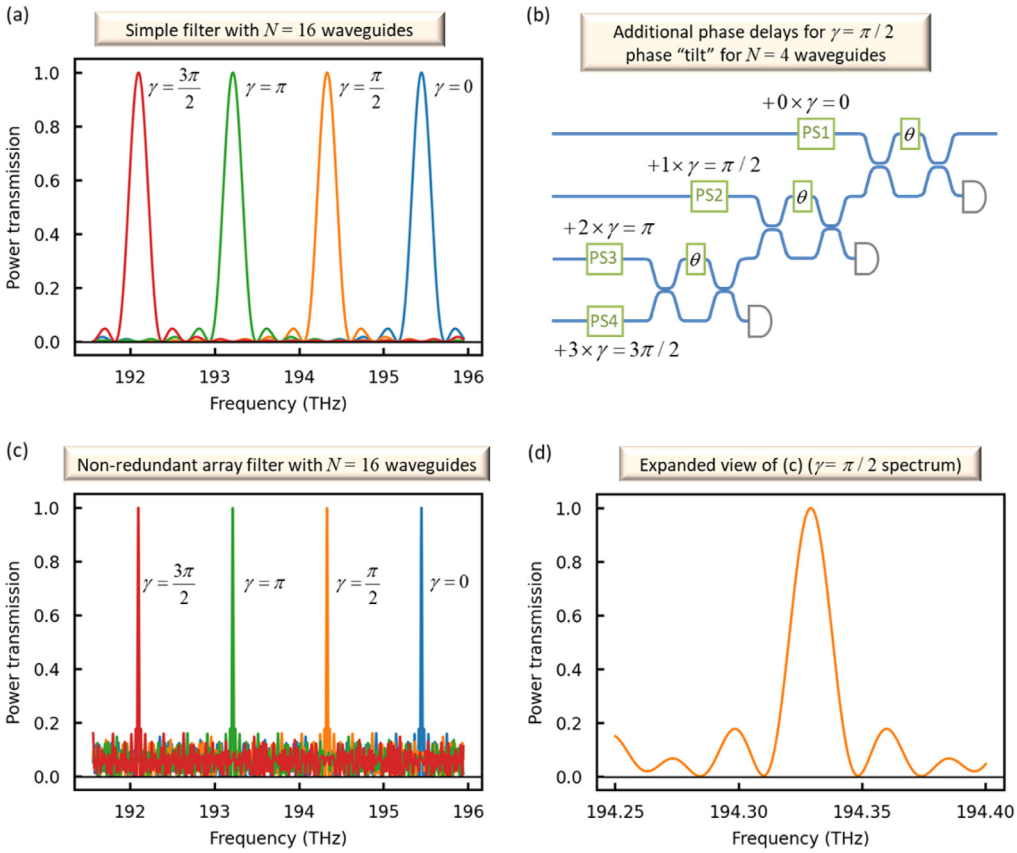


**Fig. 3.** (a), (c), and (d) Frequency response graphs for a single-layer filter with $N = 16$ waveguides in the array, designed to operate usefully over a frequency range approximately equivalent to the telecommunications C-band (1530 to 1565 nm). Waveguide lengths differ by increments of $\delta l_o = 16.51$ μm. The filter can be tuned by adding a phase "tilt" given by the tuning parameter $\gamma$ times the number $m_p$ of incremental length units $\delta l_o$ for that $P$th waveguide. Four example values of $\gamma$ are shown in (a) and (c). (b) shows the additional phase delays for $\gamma = \pi/2$ for the simpler case of $N = 4$ waveguides [as in the diagonal line mesh of Fig. 1(c) with phase shifters PS1 to PS4]. (a) Response for a simple filter where successive waveguides are longer by $\delta l_o$ than the preceding one (as in an AWG). (c) Response for a filter based on a non-redundant array of waveguide lengths that are longer by increments (based on a Golomb ruler) of [0, 1, 4, 11, 26, 32, 56, 68, 76, 115, 117, 134, 150, 163, 168, 177]$\delta l_o$. (d) The curve for the response of the as in (b) for a tuning parameter of $\gamma = \pi/2$, plotted over a narrower frequency range to show the detail of the peak response.

(see, e.g., [1] pp.177 et seq.), as may be immediately obvious from the "diagonal line" architecture; any relative complex amplitudes of tap weights can be directly programmed into the diagonal line of MZIs. Hence, various design methods [1], including matched filters, can be directly applied and programmed. (Such programming can also be simply remapped for use with (symmetric) binary tree or other self-configuring layer architectures [14].) Applications of such filters in telecommunications, for example, include dispersion compensation and gain equalization [1].

## 5. NON-REDUNDANT ARRAY SINGLE-LAYER FILTER

Many applications require narrow filter linewidths while also having a moderately large free-spectral range—for example, so that one spectral line can be distinguished or separated from a large number of others. Generally, narrow linewidths in optical spectrometers or filters require long path lengths or path length differences. High finesse resonators provide large effective path lengths because the light effectively makes many passes through the resonator, but tuning narrow resonances over large wavelength ranges can be challenging in integrated devices. Long path lengths are possible in waveguides, and long AWGs can show narrow effective linewidths [25]. However, physically defining the different waveguide lengths to high precision can be challenging, and large numbers of waveguides are required if the free-spectral range is to be a correspondingly large number of linewidths. Self-configuration of a simple filter interferometer mesh as discussed above can avoid the necessity of very precise fabrication of waveguide lengths because it automatically compensates for small errors in phase delay in different guides. However, using a large number of waveguides so that we could still have a large free-spectral range would require a correspondingly large number of interferometers, increasing complexity and physical size.

We propose a different approach to narrow linewidth and large free-spectral range, one that requires only relatively small numbers of waveguides, and that is well suited to our architecture. A key to this approach is that the waveguide lengths are no longer uniformly spaced. With careful choices of lengths, the filter can have both narrow linewidths and a broad free-spectral range; the filter peak can even be continuously tunable. The price to pay is only that the rejection of other wavelengths is not perfect.

One strategy for choosing the waveguide lengths, a so-called non-redundant array (NRA) [27–31], is already well known for spatial arrays, such as microwave antenna arrays for measuring arrival direction in radar signals [30], in spatial interferometric

approaches in astronomy [29], or in optical phased arrays [28]. The idea of an NRA in spatial applications is that the spacing between any pair of elements (such as antennas) is different from the spacing between any other pair of elements. As a result, the interference pattern formed from any two elements has a different spatial frequency (or, in two dimensions, **k** vector) from that from any other pair. Hence, generally, these interference patterns tend mostly not to add constructively. However, we can choose the phase of all the antennas so that, in one chosen direction, the result is constructive. The result is a strong (angular) peak whose width tends to be given essentially by the largest antenna separation, even though we are using only a sparse array of actual antenna elements. The price for this is that there is some generated or detected signal in the other directions, though this may be much weaker, especially as the number of antennas (or, in our case, waveguides) is increased.

In one dimension, one approach for generating NRA separations is a so-called Golomb ruler [27,32–34]. An example Golomb ruler with four markings, at positions 0, 1, 4, and 6, has different separations between any different pairs of markings. For example, 0 and 1 are obviously separated by 1 unit, 4 and 6 by 2 units, 1 and 4 by 3 units, and so on. (In this, "perfect" Golomb ruler case, all integer separations from 1 to 6 exist.)

Here, we exploit this idea in the spectral domain for optical filters. (Incidentally, the first proposal of the NRA concept was in the spectral domain for avoiding intermodulation at radio frequencies [27].) Our waveguides now have lengths set by such an NRA principle, but the architecture is otherwise the same as in Fig. 1. This approach allows a strong and narrow spectral peak, albeit accompanied by some finite transmission at other wavelengths.

Figure 3(c) shows example behaviors for a device with a set of 16 waveguides of relative lengths $m_p \delta l_o$ with the $m_p$ values for successive waveguides being the successive elements of the (Golomb ruler) set of integers {0, 1, 4, 11, 26, 32, 56, 68, 76, 115, 117, 134, 150, 163, 168, 177}, where we use the same $\delta l_o = 16.51$ μm as for Fig. 3(a). Figure 3(d) shows the curve for $\gamma = \pi/2$ at finer frequency resolution to show the character of the peak response more clearly.

The frequency when all waveguide outputs are added in phase by the mesh corresponds to the peak of the spectral response. In an ideal loss-less case, all the power at that frequency is coupled to the signal output waveguide, and this response can also be self-configured as before when shining in the frequency of interest. Though we have chosen explicitly non-redundant sets of integers to define waveguide lengths, one could also likely get a similar response with other, and possibly non-integer, lengths provided those lengths spanned a similar set of waveguide lengths, possibly even in a somewhat random fashion.

We see that this approach would allow very narrow bandwidths and wide free-spectral range even with limited numbers of waveguides, at the expense of limited rejection of other wavelengths. It is well suited to our approach that can compensate automatically for minor fabrication errors in phase delay (especially in long waveguides) and allows simple tunability.

## 6. MULTILAYER FILTERS

### A. Unitary Multilayer Filters

By adding more interferometer mesh layers, as in Fig. 2, we can program up to $N$ orthogonal filter functions to give corresponding outputs in the signal output of the corresponding layer. All filter functions, one from each layer, are available simultaneously, without any loss beyond the basic background losses of the system—that is, with no additional "splitting" loss. Even with unequally spaced waveguide lengths, as in the non-redundant array filter above, we can still losslessly and simultaneously form filter functions up to any $N$ orthogonal linear combinations of the corresponding Fourier-like basis functions $h_p(\delta\omega)$ as in Eq. (4).

Because of the construction of the multilayer unitary filter, the multiple filter functions it implements are physically guaranteed to be orthogonal to one another (at least if the mesh is "perfect"—that is, with 50:50 beam beamsplitters and the same loss on all paths through the mesh, a condition that can be arranged even with imperfect fabricated devices [13,26]); each such filter function corresponds to a different row of a unitary matrix, and such rows are necessarily orthogonal (see Supplement 1, Section S1 for discussion of orthogonality). See Supplement 1, Section S3 for an extended discussion and self-configuring and programming approaches.

For example, with an $N = 16$ waveguide design as in the single-layer simple filter above [Fig. 3(a)], but extended to a 15-layer mesh, we could have 16 filter responses, each like the filter response of, say, the $\gamma = 0$ design in Fig. 3(a), but shifted to be equally spaced throughout the spectral range of the filter. Each such filter peak would line up spectrally with the various zeros of every other filter response. This kind of filter would correspond to the usual outputs of a corresponding AWG filter. Note though, that we could arbitrarily choose which such filter response appeared out of which output. So, in general, unlike an AWG, we could also perform an arbitrary permutation of the channels among the outputs, allowing the device also to function as a switch. Quite generally, any set of up to $N$ orthogonal filters formed from the Fourier-like basis set $h_p(\delta\omega)$ as in Eq. (4) is possible, opening a wide range of simultaneous filter functions.

### B. Rejection Filter

One interesting multilayer filter would be a rejection filter designed to eliminate one or more wavelengths from a spectrum; for example, one might want to eliminate a laser line in Raman spectroscopy. We could, for example, self-configure the first row of the mesh by shining in the frequency to be eliminated. In an ideal mesh, all that light would then be coupled out of the first signal output of the mesh. Non-idealities would limit the rejection possible this way, but the use of "perfect" MZIs [13,26,35] and related techniques is promising for high rejection ratios (e.g., >80 dB in first experiments in meshes for spatial applications [35]). The remaining light would then pass into subsequent layers for further spectral analysis. Of course, that first layer, because its spectral response cannot be infinitely sharp, would also remove some light at other frequencies, which would somewhat distort the remaining spectra. The use of a non-redundant array, as in Fig. 3(b), could allow spectrally sharp filtering of light to be rejected, at the cost of some loss and a significant and "rough" nonuniformity in the remaining spectral response.

One could use the multiple layers in the mesh to filter out multiple different frequencies. With the first layer configured to remove essentially all of some frequency $f_1$, incident light at some other frequency $f_2$ would then presumably mostly pass through into the second layer. That second layer could then be configured to remove essentially all the remaining power at frequency $f_2$. Note that these two layers, taken together, can remove all the power of any two such

frequencies. (They do not necessarily separate all of frequency $f_2$ to the second output—some of that frequency may also emerge from the output of the first layer—but all the power at both frequencies will be removed.)

We could proceed similarly through other layers of the mesh. A full mesh, with $N-1$ layers and $N$ input waveguides, could remove any $N-1$ frequencies from the spectrum; the remaining spectrum would emerge from the $N$th waveguide. Note this technique can be used for any $N-1$ frequencies in the free-spectral range, at the cost of some spectral nonuniformity and loss in the remaining transmitted light in the $N$th waveguide.

Such programmable filters could be used to block or separate out specific wavelengths. For example, in astronomy, we may want to block light-polluting sodium or mercury lines from street lights, and block or separate various specific atomic lines, such as hydrogen alpha or beta. Importantly, the filter could be tuned for different such rejections or separations—the filter function need not be fixed. Note, the light filtered this way is still available for analysis; it is not absorbed but rather separated out. By calibrating the device, specific spectral line positions or red shifts could also be measured.

### C. Non-Unitary Multilayer Filter

We can implement fully programmable non–unitary matrices $M$–for example, using the singular-value decomposition (SVD) architecture [9] of two unitary meshes with a line of modulators between them (see Supplement 1, Section S3 for an extended discussion). Then we can implement multiple non-orthogonal filtering functions simultaneously on the same incoming light.

Such an architecture obviously cannot violate the basic laws of physics. Unless we incorporate gain in the mesh (e.g., adding that to the modulation mechanism), we cannot, for example, have two different filter functions that transmit 100% of the input light at the same frequency to two different outputs at the same time. In matrix terms, without gain no singular value in the decomposition can exceed unity in magnitude. We can, however, simply rescale any desired matrix by dividing it by its largest singular value; in that rescaled case, arbitrary sets of non-orthogonal filter functions are possible, at least to the extent they can be represented on the Fourier-like basis as in Eq. (3). We should, however, expect some overall loss in such non-orthogonal filters—power is formally "dumped" in the modulators that represent singular values of magnitude less than unity. See Supplement 1, Section S3 for an extended discussion.

## 7. MEASUREMENT OF THE TEMPORAL COHERENCY MATRIX

Light that contains a range of frequencies—such as continuous spectra from a thermal light source, a light-emitting diode, or some kinds of laser pulses—can usefully be described as (temporally) partially coherent. Such partial coherence is well understood theoretically (e.g., Ref. [36]). The mode amplitude $x(t)$ in a single-mode waveguide, such as the input waveguide in Fig. 1(a), can then be described in terms of its (temporal) mutual coherence function $\Gamma(t_1, t_2)$ for any two times $t_1$ and $t_2$. For stationary processes, this function depends only on the time difference $\tau = t_1 - t_2$, and for ergodic processes, what would formally be an ensemble average of over a statistical ensemble of possible functions $x(t)$ can instead be evaluated as a time average. Such stationarity and ergodicity are typically assumed for partially coherent light [36]. Then, formally,

$$\Gamma(\tau) = \left\langle x^*(t) x\,(t+\tau) \right\rangle_t, \tag{8}$$

where $\langle \cdot \rangle_t$ denotes averaging over time $t$. With relative waveguide time delays that can be written as $p\delta t_o$ for waveguide $p$ in an AWG-like waveguide array of $N$ waveguides, we then have access to $\tau$ values of the form $(s-p)\delta t_o$ for the relative time delay between waveguide $s$ and waveguide $p$. So, we can also write $\Gamma$ in the form of a "coherency matrix" with matrix elements:

$$\Gamma_{ps} \equiv \Gamma\left((s-p)\,\delta t_o\right). \tag{9}$$

If we can establish these matrix elements for the field, then we have evaluated the (temporal) mutual coherence function, at least at the discrete set of points in time delay allowed as the integers $s$ and $p$ range from 1 to $N$.

Just as for other filter functions, the waveguide array has essentially mapped from a vector of amplitudes separated in time to a vector of amplitudes in space, in the different mesh input waveguides. Some of us previously showed how to measure the (spatial) coherency matrix of a light field using a multiple-layer self-configuring mesh [19] as in Fig. 2, sequentially optimizing the output powers in successive layers. We can now take a similar approach to measuring this temporal coherency matrix and hence the mutual coherence function. Effectively, we map temporal coherence, which can loosely be described as the degree to which light amplitudes at different times could interfere with one another, to spatial coherence, which equivalently asks how light amplitudes at different points in space or in different waveguides could interfere with one another.

We repeat the essence of the previous approach [19]. We first adjust the elements in the first mesh layer to maximize the power in its signal output. This will have established and measured the first eigenfunction of the coherency matrix; the signal output power will be the first (largest) eigenvalue, and the settings of the interferometers in the layer give the corresponding eigenvector. We proceed similarly through the successive mesh layers, establishing all the eigenvectors and eigenvalues in decreasing order. By this means, we have effectively measured the entire coherency matrix as in Eq. (9). (In addition, the use of a non-redundant array of waveguide lengths would allow us to measure the mutual coherence for a larger number of different time delays with the same number of physical measurements.) We have also physically separated the partially coherent field into its mutually incoherent and orthogonal components, presenting these as the signal output powers. (This formally corresponds to separating the field into its Karhunen–Loève expansion.) We are not aware of another approach that both measures the mutual coherence and separates it physically into these components. This separation is also non-destructive; once set up, all the subsequent light passes through from the input to the outputs. A detailed derivation of this approach and the non-redundant extension can be found in Supplement 1, Section S4.

## 8. OTHER FILTER MODALITIES AND EXTENSIONS

Because of the flexible programmability of this filter approach and the further possibilities allowed by self-configuration, there are many additional possible operating modes. There are also some extensions we can make to the physical architecture. Here

we mention some of these briefly, with an extended discussion in Supplement 1, Section S5.

(a) The device can be run backwards for (i) wavelength multiplexing, (ii) as a tunable mirror—e.g., as a laser tuner, or (iii) as a pulse shaper or generator.

(b) When operated for separating partially coherent fields, the device can (i) automatically separate high-coherence sources (such as light from different lasers), sharp spectral lines, or different wavelength channels, without prior knowledge of their wavelengths, and (ii) can look for and measure absorption lines or spectra against a uniform background light.

(c) The architecture of the device can be extended or modified in several ways. (i) Though we have mostly discussed either single-layer devices or complete unitary meshes with $N$ mesh input waveguides, the device can operate with fewer—say, $Q$—layers, allowing a less complicated photonic circuit while still usefully separating $Q$ wavelengths at high resolution, for example. (ii) Though we have discussed self-configuration based on power optimization, optimization on other measurable parameters is possible, with one interesting example being to optimize based on "eye-opening" or minimum bit-error rate in telecommunication systems, which could effectively construct or self-configure optimum matched filters. (iii) Though we show a fixed power splitter in Figs. 1 and 2, a controllable power splitter could be substituted, which could be useful when operating with waveguides of very different lengths (and hence different losses). (iv) Components in the meshes will not generally be perfect; such imperfections can be compensated and/or rejection improved by using "perfect" MZI approaches or the use of multiple layers for a given rejection [13,26,35]. (v) By dithering waveguide phase shifts with small modulations, the device can perform derivative spectra, which is often a useful mode for weak signals or for rejecting background. Finally, (vi) by using multiple input waveguides, each with its own waveguide array, all feeding into one or more larger mesh(es), combined spatial and spectral operation is possible simultaneously, as might be interesting for compensating modal dispersion, for example.

## 9. DISCUSSION

In a fair comparison to conventional AWG filters, when our approach is configured as a simple filter, as in the results of Fig. 3(a), the filtering performance is essentially the same as that of an AWG with similar waveguides. Also, some previous AWG approaches [8] have already proposed some degree of programmability and tunability based on a set of phase shifters in the waveguides. Furthermore, our approach requires significant added complexity in the many MZIs in the photonic circuit. Though the electronics required to drive MZI phase shifters and handle photodetector relative power measurements is relatively standard, and the algorithms for calibration and control are relatively simple and progressive, such driving, detecting, and control circuitry obviously adds complexity to the system. (See Ref. [37] for discussion of scaling the electronic circuitry and Ref. [38] for integrated approaches.) The use of thermal phase shifters in most current foundry-fabricated MZI mesh circuits involves power dissipation of tens of milliwatts, e.g., ∼22 mW for $\pi$ phase shift [39]. With one phase shifter requiring $\pi$ range and the other $2\pi$, the average power dissipation per MZI would be (at half range in each case) ∼33 mW. A simple filter with 16 waveguides (so 15 MZIs) would therefore have ∼ 0.5 W of power dissipation. A full 16 input triangular mesh (for 15 separate filter functions) would have 120 MZIs, so a power dissipation of ∼4 W. Generally, that dissipation is of course significant, but is not likely a sufficiently large number that it prevents reasonable implementations, at least for moderate numbers of waveguides (e.g., 16) and filter layers. The ideas presented here should continue to work if we can move to other phase-shifter implementations, such as micromechanical approaches or electro-optical or piezoelectric implementations, all of which avoid such power dissipation. Because of that additional control circuitry complexity and phase-shifter power dissipation, the use of large numbers of AWG waveguides, as used in high-performance AWG circuits, could be technologically challenging or limiting in our approach.

Use of thermal phase shifters can result in thermal crosstalk in setting MZIs. Use of thermally isolating trenches and algorithmic approaches, such as eigenfunction techniques [40], and/or rerunning the setup algorithms a few times to obtain convergence in the presence of moderate thermal crosstalk can mitigate such effects.

Generally, for ideal performance of MZI meshes, 50:50 splitting in the fabricated MZI beamsplitters is required; without that, perfect "cross" state behavior is not possible (see, e.g., [14]), which would in principle limit the performance of our filtering approach. First, however, we note that "double" or "perfect" MZIs [13,26] can guarantee effective 50:50 behavior at a given wavelength. Also, recent work [41] has shown fabricated splitters with similar split ratios over wide wavelength ranges. Second, our approach has approximately equal power splitting among all the mesh input waveguides. As a result, even in a worst case with a 16 waveguide system using the "diagonal line" MZI mesh architecture, the "last" MZI in the line has to combine a power of 15 units in one waveguide with 1 unit of power from another waveguide, which is equivalent to asking the MZI to have at least a 1:15 rejection ratio, the equivalent of ∼12 dB rejection. Fabricated MZIs in silicon photonics can typically have much greater than 20 dB rejection ratio, so such a ∼12 dB ratio is easily accessible. So, our approach is relatively tolerant to fabrication variations in MZI beamsplitters.

The use of the MZI mesh will also introduce additional loss compared to an AWG, though these need not be large for moderate sizes of circuits. Losses in silicon photonics directional couplers can be as low as ∼0.03 dB per coupler [41]. Propagation loss in silicon photonics foundry-fabricated waveguides can be below 0.1 dB/cm [42]. For a total waveguide length of ∼800 microns in an MZI (so a propagation loss of 0.008 dB), the total loss could therefore be as low as 0.07 dB per MZI. Even in an architecture with a diagonal line of 15 MZIs (for 16 waveguides), the loss could therefore be ∼1 dB. Even in a full 16-input triangular mesh, no path is longer than 15 MZIs, so this also represents the scale of loss in such a full mesh. In a single (symmetric) binary tree of MZIs for 16 waveguides, which would have four successive MZIs in each path, the loss could therefore be ∼0.28 dB.

We believe, however, that our approach offers many potential benefits for filtering and spectroscopy more broadly, justifying the additional complexity beyond conventional AWGs. The benefits of our approach lie in several areas.

First, it offers a broad range of different filter functions. Even the simple single-layer filter can implement any finite-impulse response filter (e.g., transversal, tapped-delay-line, or matched filters) that is based on the set of time delays of the waveguides. (Such

flexibility contrasts with resonator filters, which tend to have fixed and limited Q-factors and linewidths.) Design can be as simple as the Fourier decomposition of the desired filter function. Multilayer meshes allow multiple simultaneous filtering functions, each of which can be arbitrarily set across the range of possible filters, with no additional fundamental or "splitting" loss introduced for simultaneous orthogonal filters. (Only non-orthogonal filters necessarily require some additional loss.) All the filters are fully tunable over an entire free-spectral range, requiring only the same phase shifters used for the basic programmability of the mesh.

Second, filter functions can be automatically discovered by self-configuring to the input light. For a single input wavelength, simple progressive algorithms can set a mesh layer to filter exactly that wavelength, without any prior knowledge of the wavelength. By leaving the configuration algorithm running, the filter can automatically track that wavelength if it changes for any reason. Equivalently, periodically recalibrating with a reference wavelength can hold or reset the device behavior even in the presence of environmental changes (e.g., temperature) or component aging. Such a single wavelength input also allows simple calibration of the set of waveguides and the entire set of mesh layers by completely progressive algorithms based only on power minimization or maximization in a detector or detectors [14,43]. Such calibration also allows automatic compensation for fabrication errors in the precise phase delays or lengths of waveguides and any other static phase shifts, allowing possibly very long waveguide lengths for precise spectral filtering. Operating using self-configuration algorithms [9,12–14,43] also automatically compensates for such phase-delay errors. Variations in loss in different waveguide paths can also be automatically compensated by the mesh layers. Pre-compensation with a programmable power splitter allows simple filter analysis and programming even with substantially different losses in different waveguides. (In this case, the spectral resolution of the filter is not limited by losses in the waveguides.)

Third, this can be a universal filter approach that is software-defined and is completely programmable and reprogrammable in the field with simple progressive algorithms.

Fourth, this approach offers novel operation modalities. In an $N$ waveguide device, up to $N-1$ wavelengths lying anywhere in the filter's free-spectral range can be completely and automatically rejected from the remaining output. Our additional novel concept of a non-redundant array filter allows very narrow and programmable spectral response even with only moderate numbers of waveguides and circuit complexity, at the expense only of finite rejection at other wavelengths. The use of multilayer meshes together with algorithms that maximize (or minimize) power over an entire mesh layer at once allows powerful functions operating on partially coherent light, including separation into its mutually temporally incoherent components (a physical Karhunen–Loève decomposition). This approach allows measurement of the temporal coherence function; we are not aware of any other approach that accomplishes either this physical separation or this non-destructive measurement of temporal coherence. It also enables functionalities such as absorption spectroscopy in the presence of a broad background spectrum.

## 10. CONCLUSION

In conclusion, the approach to spectral filtering presented here, by exploiting the programmability of interferometer meshes together with waveguide arrays, offers a wide range of filters and operational modalities. Multiple simultaneous filters are possible. All these filter functions can be programmed and re-programmed after fabrication and can exploit the self-configuring possibilities of forward-only meshes formed from self-configuring layers to set themselves up optimally based on the input light. Some of the resulting capabilities, such as measurement and separation of partially coherent light fields, are apparently beyond previous optical systems. The approach also offers tolerance to fabrication variations, self-calibration, and self-stabilization. Taken together, these features and capabilities are very promising for future integrated photonic filters and spectrometers.

**Funding.** Air Force Office of Scientific Research (FA9550-21-1-0312, FA9550-23-1-0307); Stanford University (Stanford Science Fellowship); Stanford University (Texas Instruments Stanford Graduate Fellowship); Stanford University (John and Kate Wakerly Stanford Graduate Fellowship); National Science Foundation (Graduate Research Fellowship Program); HORIZON EUROPE European Research Council (101067268); National Aeronautics and Space Administration (Early Career Initiative (ECI) program).

**Disclosures.** The authors declare no conflicts of interest.

**Data availability.** Data underlying the results presented in this paper are not publicly available at this time but may be obtained from the authors upon reasonable request.

**Supplemental document.** See Supplement 1 for supporting content.

## REFERENCES

1. C. K. Madsen and J. H. Zhao, *Optical Filter Design and Analysis: A Signal Processing Approach Wiley* (1999).
2. M. K. Smit, "New focusing and dispersive planar component based on an optical phased array," Electron. Lett. **24**, 385–386 (1988).
3. H. Takahashi, S. Suzuki, K. Kato, *et al.*, "Arrayed-waveguide grating for wavelength division multi/demultiplexer with nanometre resolution," Electron. Lett. **26**, 87–88 (1990).
4. C. Dragone, "An N*N optical multiplexer using a planar arrangement of two star couplers," IEEE Photon. Technol. Lett **3**, 812–815 (1991).
5. K. Okamoto, K. Takiguchi, and Y. Ohmori, "16-channel optical add/drop multiplexer using silica-based arrayed-waveguide gratings," Electron. Lett. **31**, 723–724 (1995).
6. E. J. Stanton, N. Volet, and J. E. Bowers, "Low-loss demonstration and refined characterization of silicon arrayed waveguide gratings in the near-infrared," Opt. Express **25**, 30651–30663 (2017).
7. F. Kish, V. Lal, P. Evans, *et al.*, "System-on-chip photonic integrated circuits," IEEE J. Sel. Top. Quantum Electron **24**, 1–20 (2018).
8. M. S. Rasras, I. Kang, M. Dinu, *et al.*, "A programmable 8-bit optical correlator filter for optical bit pattern recognition," IEEE Photon. Technol. Lett **20**, 694–696 (2008).
9. D. A. B. Miller, "Self-configuring universal linear optical component," Photon. Res. **1**, 1–15 (2013).
10. W. Bogaerts, D. Pérez, J. Capmany, *et al.*, "Programmable photonic circuits," Nature **586**, 207–216 (2020).
11. D. Pérez-López, A. Gutierrez, D. Sánchez, *et al.*, "General-purpose programmable photonic processor for advanced radiofrequency applications," Nat. Commun. **15**, 1563 (2024).
12. D. A. B. Miller, "Self-aligning universal beam coupler," Opt. Express **21**, 6360–6370 (2013).
13. D. A. B. Miller, "Perfect optics with imperfect components," Opt. **2**, 747–750 (2015).
14. D. A. B. Miller, "Analyzing and generating multimode optical fields using self-configuring networks," Optica **7**, 794–801 (2020).
15. S. Pai, I. A. D. Williamson, T. W. Hughes, *et al.*, "Parallel programming of an arbitrary feedforward photonic network," IEEE J. Sel. Top. Quantum Electron **26**, 1 (2020).
16. A. Annoni, E. Guglielmi, M. Carminati, *et al.*, "Unscrambling light—automatically undoing strong mixing between modes," Light Sci. Appl. **6**, e17110 (2017).
17. M. Milanizadeh, F. Toso, G. Ferrari, *et al.*, "Coherent self-control of free-space optical beams with integrated silicon photonic meshes," Photon. Res. **9**, 2196–2204 (2021).

18. M. Milanizadeh, S. SeyedinNavadeh, F. Zanetto, *et al.*, "Separating arbitrary free-space beams with an integrated photonic processor," Light Sci. Appl. **11**, 197 (2022).
19. C. Roques-Carmes, S. Fan, and D. A. B. Miller, "Measuring, processing, and generating partially coherent light with self-configuring optics," Light Sci. Appl. **13**, 260 (2024).
20. S. SeyedinNavadeh, M. Milanizadeh, F. Zanetto, *et al.*, "Determining the optimal communication channels of arbitrary optical systems using integrated photonic processors," Nat. Photonics **18**, 149–155 (2024).
21. A. Ribeiro, A. Ruocco, L. Vanacker, *et al.*, "Demonstration of a $4 \times 4$-port universal linear circuit," Optica **3**, 1348–1357 (2016).
22. S. Pai, Z. Sun, T. W. Hughes, *et al.*, "Experimentally realized in situ backpropagation for deep learning in photonic neural networks," Science **380**, 398–404 (2023).
23. J. Bütow, J. S. Eismann, J. S. Eismann, *et al.*, "Spatially resolving amplitude and phase of light with a reconfigurable photonic integrated circuit," Optica **9**, 939–946 (2022).
24. S. Pai, C. Valdez, T. Park, *et al.*, "Power monitoring in a feedforward photonic network using two output detectors," Nanophotonics **12**, 985–991 (2023).
25. K. Okamoto, "Progress and technical challenge for planar waveguide devices: silica and silicon waveguides," Laser Photonics Rev. **6**, 14–23 (2012).
26. C. M. Wilkes, X. Qiang, J. Wang, *et al.*, "60 dB high-extinction auto-configured Mach–Zehnder interferometer," Opt. Lett. **41**, 5318–5321 (2016).
27. W. C. Babcock, "Intermodulation interference in radio systems frequency of occurrence and control by channel selection," Bell Syst. Tech. J. **32**, 63–73 (1953).
28. T. Fukui, R. Tanomura, K. Komatsu, *et al.*, "Non-redundant optical phased array," Optica **8**, 1350–1358 (2021).
29. G. Perrin, S. Lacour, J. Woillez, *et al.*, "High dynamic range imaging by pupil single-mode filtering and remapping," Mon. Not. R. Astron. Soc. **373**, 747–751 (2006).
30. A. Ahmed and Y. D. Zhang, "Generalized non-redundant sparse array designs," IEEE Trans. Sig. Proc. **69**, 4580–4594 (2021).
31. N. Anselmi, A. Melloni, F. Morichetti, *et al.*, "On the design of unconventional optical phased array antennas," in *17th European Conference on Antennas and Propagation (EuCAP)* (2023).
32. S. W. Golomb, "How to number a graph," in *Graph Theory and Computing*, R. C. Read, ed. (Academic Press, 1972), pp. 23–37.
33. M. Gardner, "Mathematical games–the graceful graphs of Solomon Golomb, or how to number a graph parsimoniously," Sci. Am. **226**, 108–112 (1972).
34. G. S. Bloom and S. W. Golomb, "Applications of numbered undirected graphs," Proc. IEEE **65**, 562–570 (1977).
35. D. Sirbu, R. Belikov, K. Fogarty, *et al.*, "AstroPIC: near-infrared photonic integrated circuit coronagraph architecture for the Habitable Worlds Observatory," Proc. SPIE **13092**, 553–565 (2024).
36. J. W. Goodman, *Statistical Optics*, 2nd edition (Wiley, 2015).
37. F. Zanetto, M. Milanizadeh, F. Morichetti, *et al.*, "Scalable techniques for electronic control of programmable photonic circuits," in *IEEE Photonics Conference (IPC)* (2024).
38. F. Zanetto, F. Toso, M. Crico, *et al.*, "Unconventional monolithic electronics in a conventional silicon photonics platform," IEEE Trans. Electron Dev. **70**, 4993–4998 (2023).
39. M. Jacques, A. Samani, E. El-Fiky, *et al.*, "Optimization of thermo-optic phase-shifter design and mitigation of thermal crosstalk on the SOI platform," Opt. Express **27**, 10456–10471 (2019).
40. M. Milanizadeh, S. Ahmadi, M. Petrini, *et al.*, "Control and calibration recipes for photonic integrated circuits," IEEE J. Sel. Top. Quantum Electron. **26**, 1–10 (2020).
41. A. Bayoumi, M. Oktay, A. Elshazly, *et al.*, "Enhanced operation range of silicon MZI filters using a broadband bent directional coupler," IEEE Photonics Technol. Lett. **37**, 501–504 (2025).
42. D. Onural, H. Gevorgyan, B. Zhang, *et al.*, "Silicon waveguides and resonators with Sub-0.1 dB/cm propagation loss and over 7 million Q in a foundry process," in *Frontiers in Optics + Laser Science 2021* (Optica Publishing Group, 2021), paper FTh6B.4.
43. D. A. B. Miller, "Setting up meshes of interferometers; reversed local light interference method," Opt. Express **25**, 29233–29248 (2017).